Submitted to Physics of Fluids

RECEIVED
LAWRENCE
RADIATION LABORATORY

NOV 13 1970

LIBRARY AND
DOCUMENTS SECTION

UCRL-20066
Preprint

c.2

EXACT NONLINEAR EVOLUTION OF ALFVÉN MODES IN THE GUIDING-CENTER MODEL

Blake Patterson

August 14, 1970

AEC Contract No. W-7405-eng-48

TWO-WEEK LOAN COPY

This is a Library Circulating Copy which may be borrowed for two weeks. For a personal retention copy, call Tech. Info. Division, Ext. 5545

UCRL-20066 c.2

LAWRENCE RADIATION LABORATORY
UNIVERSITY of CALIFORNIA BERKELEY

77

DISCLAIMER

This document was prepared as an account of work sponsored by the United States Government. While this document is believed to contain correct information, neither the United States Government nor any agency thereof, nor the Regents of the University of California, nor any of their employees, makes any warranty, express or implied, or assumes any legal responsibility for the accuracy, completeness, or usefulness of any information, apparatus, product, or process disclosed, or represents that its use would not infringe privately owned rights. Reference herein to any specific commercial product, process, or service by its trade name, trademark, manufacturer, or otherwise, does not necessarily constitute or imply its endorsement, recommendation, or favoring by the United States Government or any agency thereof, or the Regents of the University of California. The views and opinions of authors expressed herein do not necessarily state or reflect those of the United States Government or any agency thereof or the Regents of the University of California.

EXACT NONLINEAR EVOLUTION OF ALFVÉN MODES IN THE GUIDING-CENTER MODEL*

Blake Patterson

Lawrence Radiation Laboratory
University of California
Berkeley, California 94720

August 14, 1970

ABSTRACT

Alfvén waves parallel to a uniform magnetic field in a uniform but anisotropic plasma are studied in the CGL and guiding-center models. Exact solutions are found in the stable and unstable cases. When the plasma is stable, an arbitrarily large constant amplitude perturbation perpendicular to the uniform field can propagate without distortion parallel to the uniform field. The exact nonlinear behavior of an unstable circularly polarized Alfvén mode is obtained: growth of a finite perturbation is quenched in a finite time, and decay begins immediately.

I. INTRODUCTION

Energy conservation prevents the indefinite growth of a linearly unstable plasma wave. Nonlinear effects, such as wave-particle and wave-wave interactions, ultimately limit the amplitude of modes that increase exponentially with time in linear theory.

This mode quenching problem rarely yields analytic solutions in simple closed form, and insight regarding wave-saturation processes is acquired with difficulty. Except in special cases, even the qualitative properties are unknown. For example, does the plasma approach the saturated state of maximum wave energy asymptotically as $t \to \infty$, or does saturation occur in a finite time? If the latter holds, does the quenched state represent a stable configuration, or will further evolution occur?

In preparation for a more detailed nonlinear analysis of low-frequency waves, it was discovered that the circularly polarized Alfvén wave oriented parallel to a uniform magnetic field in a uniform anisotropic plasma is an exact solution of both the Chew-Goldberger-Low (CGL) equations[1] and the guiding-center (GC) equations.[2,3] When an excess of pressure parallel to the magnetic field makes such a wave unstable, it is known as the "firehose" or "garden-hose" instability. By use of elementary analytical methods, the nonlinear quenching of this unstable wave can be solved exactly in either model, thus providing perhaps the first simple and complete solution of the nonlinear growth of a plasma wave, rigorous within the limitations of the GC equations.

In what follows we will consider Alfvén waves in an infinite, uniform plasma in a uniform magnetic field $\underset{\sim}{B}_0$. The velocity distribution will in general be anisotropic.

The firehose mode has already been studied in such a plasma by quasilinear techniques.[4-6] The Vlasov equation carried to second order in the perturbation shows that the unstable waves, initially growing due to an excess of pressure parallel to $\underset{\sim}{B}_0$, react back on the particle distribution, causing the parallel pressure to decrease and the perpendicular pressure to increase as long as any waves are growing; the growth rate is made smaller by the relative decrease of parallel pressure, and wave growth is thus self-quenched. An explicit examination of this process has not appeared in the literature.

The CGL model was chosen for this paper primarily for the simplicity inherent in a fluid description and because to lowest order it predicts the same nonlinear behavior of Alfvén waves as the Vlasov equation. In Appendix A the earlier quasilinear results are generalized to arbitrary $\underline{k}$ by carrying the CGL equations to second order in the wave perturbation. (Of course, finite ion-gyroradius effects must be appended to the CGL equations to correctly predict growth rates for small wavelengths.) This calculation verifies that, at least to second order, the CGL model agrees with the more complete kinetic description. It was thus deemed a reasonable model for this investigation despite the approximations implicit in it.

The Alfvén modes that exactly solve the CGL model also satisfy without approximation the more widely recognized GC equations. Moreover, the GC solution has the property that the heat-flow tensor, which is

arbitrarily dropped in deriving the CGL equations, vanishes, providing further justification for the suitability of the CGL equations to this study.

Section II treats exact Alfvén wave solutions in the CGL model. In Sec. IIA a magnetic perturbation perpendicular to the uniform field $\underset{\sim}{B}_0$ of constant, but arbitrarily large, amplitude is shown to be an exact solution of the CGL equations provided the usual Alfvén wave stability criterion, Eq. (19), is satisfied. Such waves propagate without distortion parallel to $\underset{\sim}{B}_0$ at the generalized Alfvén velocity, given by Eq. (16). Figure 1 illustrates examples of this wave. The constant-amplitude Alfvén wave in the CGL model has been briefly treated as an example of a "simple wave" of classical fluid theory.[7]

In Sec. IIB a circularly polarized Alfvén wave with $\underset{\sim}{k}$ parallel to $\underset{\sim}{B}_0$ is studied. This mode reduces the CGL model to the simple Eqs. (12), (13), (20), and (23) through (27), which are derived without any approximations. The mode does not propagate. The magnetic field has a helical structure consisting of $\underset{\sim}{B}_0$ and a component perpendicular to $\underset{\sim}{B}_0$ of signed amplitude $\mathcal{b}(t)$, as shown in Fig. 2. The time evolution of $\mathcal{b}(t)$ is easily obtained from the energy Eq. (24): $\mathcal{b}(t)$ can be viewed as the displacement of a classical particle moving in the potential $\Phi(\mathcal{b})$, which is sketched in Fig. 3 for various initial plasma conditions. If the stability criterion (19) holds, $\mathcal{b}(t)$ oscillates between positive and negative values with an amplitude-dependent frequency, which approaches the Alfvén frequency in the small-amplitude limit.

If the Alfvén stability criterion (19) is not satisfied, three special cases can occur, depending on the particular boundary conditions assumed for the plasma. The usual initial condition assumed for plasma instability studies corresponds to Fig. 3(c), in which $p_{\parallel}(0) > p_{\perp}(0) + B_0^2/4\pi$, and the initial perturbation amplitude b and its time derivative $\dot{b}$ are small and positive. The amplitude grows exponentially at first, then more slowly; it reaches a maximum value in a finite time and immediately decreases, ultimately decreasing to zero exponentially. This demonstrates that wave quenching occurs in a finite time and is followed by immediate decay. If the initial conditions correspond to the situation in Fig. 3(d), the wave amplitude oscillates (nonsinusoidally), never passing through zero. If the initial conditions correspond to Fig. 3(b), the wave amplitude oscillates nonsinusoidally and passes through zero twice each period.

Section III shows that identical results are obtained from the GC equations.

In Sec. IV the exact results of Secs. II and III are discussed. It is noted that the constant-amplitude wave may be an important low-frequency phenomenon in the solar wind. The circularly polarized firehose mode is related to the quasilinear theory[4-6] of the Alfvén instability. Qualitative features of the nonlinear evolution of the circularly polarized firehose mode are compared with characteristics of other unstable waves.

II. PARALLEL ALVÉN WAVES IN THE CGL MODEL

The CGL equations or double adiabatic equations are[1,3]

$$d\rho/dt = -\rho\nabla\cdot\underset{\sim}{u}, \tag{1}$$

$$\rho d\underset{\sim}{u}/dt = -\nabla\cdot\underset{\approx}{p} + (\nabla \times \underset{\sim}{B}) \times \underset{\sim}{B}/4\pi , \tag{2}$$

$$\partial\underset{\sim}{B}/\partial t = \nabla \times (\underset{\sim}{u} \times \underset{\sim}{B}), \tag{3}$$

$$d(p_\perp \rho^{-1} B^{-1})/dt = 0, \tag{4}$$

$$d(p_\parallel B^2 \rho^{-3})/dt = 0, \tag{5}$$

$$\nabla\cdot\underset{\sim}{B} = 0, \tag{6}$$

$$\begin{aligned} \underset{\approx}{p} &= p_\perp(\underset{\approx}{I} - \hat{B}\hat{B}) + p_\parallel \hat{B}\hat{B}, \\ &= p_\perp I + p_\Delta \hat{B}\hat{B}, \end{aligned} \tag{7}$$

$$p_\Delta \equiv p_\parallel - p_\perp. \tag{8}$$

The usual notation for the convective derivative, $d/dt \equiv (\partial/\partial t + \underset{\sim}{u}\cdot\nabla)$, has been used. In these equations B denotes the magnitude of the total magnetic field $\underset{\sim}{B}$.

We assume that the unperturbed state consists of a uniform plasma in a uniform and constant magnetic field $\underset{\sim}{B}_0$. Choose a Cartesian coordinate system with z axis parallel to $\underset{\sim}{B}_0$.

All plasma waves discussed in Secs. II and III are assumed to have the following space-time dependence:[8]

$$\underset{\sim}{u} = \underset{\sim}{u}(z,t), \tag{9a}$$

$$\underset{\sim}{B} = \underset{\sim}{B}_0 + \underset{\sim}{b}(z,t), \tag{9b}$$

$$\underset{\sim}{u}\cdot\underset{\sim}{B}_0 = 0, \tag{9c}$$

$$\underset{\sim}{b}\cdot\underset{\sim}{B}_0 = 0, \tag{9d}$$

$$b \equiv |\underset{\sim}{b}(z,t)| = b(t), \tag{9e}$$

$$p_\perp = p_\perp(t), \tag{9f}$$

$$p_\parallel = p_\parallel(t), \tag{9g}$$

$$\rho = \text{constant}. \tag{9h}$$

Note that the only spatial dependence is through the variable z, hence the name parallel Alfvén waves.

Without any approximation, use of properties (9) reduces the CGL Eqs. (1) through (8) to the simple system

$$\partial\underset{\sim}{b}/\partial t = B_0\, \partial\underset{\sim}{u}/\partial z, \tag{10}$$

$$\rho\partial\underset{\sim}{u}/\partial t = -(B_0/B^2)(p_\Delta - B^2/4\pi)\partial\underset{\sim}{b}/\partial z, \tag{11}$$

$$p_\perp(t)/p_\perp(0) = B(t)/B(0), \tag{12}$$

$$p_\parallel(t)/p_\parallel(0) = B^2(0)/B^2(t). \tag{13}$$

Equations (10) and (11) can be combined to give a wave equation for $\underset{\sim}{b}$:

$$\partial^2 \underset{\sim}{b}/\partial t^2 = -\rho^{-1}(B_0/B)^2(p_\Delta - B^2/4\pi)\partial^2 \underset{\sim}{b}/\partial z^2. \tag{14}$$

Equation (14) can be treated by a separation of variables technique, but, due to its nonlinearity, particular solutions cannot be superposed to give more general ones. Guided by solutions of the linearized plasma equations, we investigate two classes of solutions of Eqs. (10) through (14).

A. Constant-Amplitude Solutions in the CGL Model

Assume $b(t)$ is constant in time. Equations (12) and (13) imply that $p_\parallel$ and $p_\perp$ are also constant. With $\underset{\sim}{b} = b\,\hat{b}(z,t)$, Eq. (14) reduces to

$$\partial^2 \hat{b}/\partial t^2 = V^2\, \partial^2 \hat{b}/\partial z^2, \tag{15}$$

where the generalized Alfvén velocity V is given by

$$V^2 = \rho^{-1}(B_0/B)^2[(B^2/4\pi) - p_\Delta] \tag{16}$$

and is also constant.

The general solution of the simple wave Eq. (15) is

$$\hat{b} = \hat{x}\cos\Theta(z - Vt) + \hat{y}\sin\Theta(z - Vt), \tag{17}$$

where $\underset{\sim}{b}$ has been chosen perpendicular to $\underset{\sim}{B}_0$ in accordance with Eq. (9d), and $\Theta(\cdot)$ is any twice differentiable real function.

For example, if $\Theta(x) \propto \tanh(kx)$, then for $|z - Vt| \gg k^{-1}$ the direction of $\underset{\sim}{b}$ is nearly constant, whereas when $|z - Vt| \lesssim k^{-1}$, $\underset{\sim}{b}$ rotates. The total magnetic field is essentially uniform where

$|z - Vt| \gg k^{-1}$ and is slanted with respect to the $\underset{\sim}{B}_0$ direction in this region. The field lines twist in the vicinity of $z = Vt$ so that the total field $\underset{\sim}{B}$ always makes the same angle with $\underset{\sim}{B}_0$. The approximate shapes of the field lines for $\Theta(x) = \pi \tanh(kx)$, $\Theta(x) = \pi/2 \tanh(kx)$, and $\Theta(x) = (7\pi/2)\exp[-(kx)^2]$ are shown in Fig. 1 (a), (b), and (c), respectively. In the CGL model, the field structures shown propagate without distortion at velocity V parallel to $\underset{\sim}{B}_0$. The propagating interface at $z = Vt$, where the interesting field behavior occurs, has been likened to a shock front moving through a uniform plasma. The helical structure of Fig. 2 results if $\Theta(x) \doteq kx$.

The fluid velocity $\underset{\sim}{u}$ is obtained from Eq. (10):

$$\underset{\sim}{u}(z,t) = -(V/B_0)\underset{\sim}{b}(z,t). \tag{18}$$

Since $\underset{\sim}{u}$ must be real, V must be real, i.e.,

$$p_{\parallel} < p_{\perp} + B^2/4\pi, \tag{19}$$

which is the well-known stability criterion for Alfvén waves.

In summary, Eqs. (16) through (18) and (9a) through (9h) constitute an exact solution of the full nonlinear CGL equations when the stability criterion (19) is satisfied. The solution is a wave of arbitrary but constant amplitude, propagating without distortion at the Alfvén velocity $|V|$, parallel or antiparallel to $\underset{\sim}{B}_0$. The total field $\underset{\sim}{B}$ always makes the same angle with $\underset{\sim}{B}_0$ and has the same orientation throughout each plane z = constant.

B. Solutions with Time-Varying Amplitudes in the CGL Model

We next consider solutions of Eqs. (10) through (14) in which the wave amplitude can vary with time.

Since Eq. (9) assumes that the wave amplitude is independent of z, we write

$$\underset{\sim}{b}(z,t) = \mathcal{b}(t)\,\hat{b}(z), \tag{20}$$

where $\mathcal{b}(t)$ represents an amplitude that may assume positive or negative values. Substitution of this trial solution into Eq. (14) gives

$$(d^2\mathcal{b}/dt^2)\hat{b} = -\rho^{-1}(B_0/B)^2(p_\Delta - B^2/4\pi)\mathcal{b}\, d^2\hat{b}/dz^2.$$

Separating this equation into parts dependent on z and t, respectively, we find

$$d^2\hat{b}/dz^2 = -k^2\hat{b} \tag{21}$$

and

$$d^2\mathcal{b}/dt^2 = k^2\rho^{-1}(B_0/B)^2(p_\Delta - B^2/4\pi)\mathcal{b}\ . \tag{22}$$

In order that $\hat{b}$ have finite components, the constant k must be real, and Eq. (21) gives:

$$\hat{b}(z) = \hat{x}\cos(kz + \delta) + \hat{y}\sin(kz + \delta). \tag{23}$$

Thus the magnetic field has a helical structure with axis parallel to $\underset{\sim}{B}_0$ as shown in Fig. 2. In what follows we assume the wavelength large compared with the ion gyroradius to preserve the validity of the CGL model.

An energy-like equation for $\mathcal{b}(t)$ can be obtained by multiplying Eq. (22) by $\dot{\mathcal{b}}$, using Eqs. (12) and (13) to carry out the resulting elementary integrations. Thus we find

$$\frac{1}{2}\dot{\mathcal{b}}^2 + \Phi(\mathcal{b}) = K, \tag{24}$$

where K is a constant and

$$\Phi(\mathcal{b}) \equiv \frac{1}{2} k^2 B_0^{\,2} \rho^{-1}\{p_{\parallel}(0)[B(0)/B]^2 + 2p_{\perp}(0)[B/B(0)] + B^2/4\pi\}. \tag{25}$$

The dependence of Φ on $\mathcal{b}$ is through B:

$$B = (B_0^{\,2} + \mathcal{b}^2)^{\frac{1}{2}}. \tag{26}$$

From Eqs. (10), (11), (20), and (23) we find

$$\underset{\sim}{u}(z,t) = (kB_0)^{-1}\dot{\mathcal{b}}\,[\hat{x}\sin(kz + \delta) - \hat{y}\cos(kz + \delta)]. \tag{27}$$

Equations (12) and (13) specify $p_{\perp}(t)$ and $p_{\parallel}(t)$.

If Eq. (18) is multiplied by $\rho(kB_0)^{-2}$, and Eqs. (12), (13), and (27) are used to simplify the result, we obtain

$$\frac{1}{2}\rho\, u^2(t) + \frac{1}{2} p_{\parallel}(t) + p_{\perp}(t) + B^2(t)/8\pi = K'. \tag{28}$$

This is the energy equation for the combined system of plasma and wave with the obvious physical interpretations: $\frac{1}{2}\rho u^2$ represents the plasma translational energy density, $\frac{1}{2} p_{\parallel}$ is the thermal energy density parallel to $\underset{\sim}{B}$, $p_{\perp}$ is the thermal energy density perpendicular to $\underset{\sim}{B}$, and $B^2/8\pi$ is the total energy density in the field.

Viewing Eq. (24) as an equation in $\mathfrak{b}(t)$, we see that it describes the motion of a particle with displacement $\mathfrak{b}$, velocity $\dot{\mathfrak{b}}$, and total energy K moving in the potential $\Phi(\mathfrak{b})$. The time development of $\mathfrak{b}(t)$ follows easily from this interpretation of Eq. (24).

First we consider the properties of $\Phi(\mathfrak{b})$. From Eq. (25), one obtains

$$\partial\Phi/\partial\mathfrak{b} \propto \mathfrak{b}\{[B_0^2/4\pi] + p_\perp(0)\, B_0^2[B(0)B]^{-1} - p_\parallel(0)\, B_0^2\, B^2(0)B^{-4}\}. \tag{29}$$

One extremum occurs at $\mathfrak{b} = 0$, because Φ is even in $\mathfrak{b}$. When multiplied by B^4 the curly brace in Eq. (29) is a monotonically increasing function of $|\mathfrak{b}|$. Thus the brace is positive for all $\mathfrak{b} \neq 0$, if it is non-negative at $\mathfrak{b} = 0$, i.e., if

$$(B_0^2/4\pi) + p_\perp(0)[B_0/B(0)] - p_\parallel(0)[B(0)/B_0]^2$$

$$= (B_0^2/4\pi) + (p_\perp)_{\mathfrak{b}=0} - (p_\parallel)_{\mathfrak{b}=0} > 0. \tag{30}$$

Equation (30) is the Alfvén stability criterion; when it holds, $\Phi(\mathfrak{b})$ has only the extremum at $\mathfrak{b} = 0$ and must have the form sketched in Fig. 3 (a). In the Alfvén unstable case, when Eq. (30) does not hold, the curly brace is zero for exactly one value of $|\mathfrak{b}| > 0$, and $\Phi(\mathfrak{b})$ must have the form sketched in Fig. 3 (b).

Evolution of the circularly polarized Alfvén wave in the stable and unstable cases is governed by the energy constant K, which is determined by the initial conditions.

Case 1. Stable Plasma

When Eq. (30) holds, $\Phi(0)$ is the minimum value of $\Phi(\mathcal{b})$. Thus K cannot be less than $\Phi(0)$, since this would imply an imaginary velocity $\dot{\mathcal{b}}$.

A quiescent, stable plasma with $\mathcal{b} = 0$ corresponds to $K = \Phi(0)$.

Assume $K > \Phi(0)$, and let $-\mathcal{b}_1 = \mathcal{b}_2 > 0$ be the real roots of the equation $\Phi(\mathcal{b}) = K$, which is a quartic in B. In view of Eq. (24) and Fig. 3(a), $\mathcal{b}$ oscillates between the turning points $\mathcal{b}_1$ and $\mathcal{b}_2$. Figure 2 shows the magnetic field behavior for this wave. One complete cycle, observed from a fixed spatial reference, is demonstrated by the sequence (a)(b)···(f)(g)(f)···(a).

When $|\mathcal{b}_{1,2}| \ll B_0$, Eq. (24) can be expanded in $\mathcal{b}$ to give

$$\frac{1}{2}\dot{\mathcal{b}}^2 + \frac{1}{2}\rho^{-1} k^2[(B_0^2/4\pi) + p_\perp(0) - p_\parallel(0)]\mathcal{b}^2 = \Delta, \quad . \tag{31}$$

where Δ is a positive constant. Equation (31) is that of a simple harmonic oscillator with its frequency ω given by

$$\omega^2 = \rho^{-1} k^2[(B_0^2/4\pi) + p_\perp(0) - p_\parallel(0)]. \tag{32}$$

Thus for small amplitude waves we recover the Alfvén dispersion relation. This solution is a standing wave; it can be viewed as a linear combination of two circularly polarized Alfvén waves, special types of the constant-amplitude solution considered in Sec. II A, propagating in opposite directions.

For more severe perturbations the frequency of oscillation is amplitude-dependent, the period τ being simply the transit time of the "magnetic" particle oscillating in the potential $\Phi(\mathcal{b})$:

$$\tau = 2\int_{\mathcal{b}_1}^{\mathcal{b}_2} \frac{d\mathcal{b}}{\dot{\mathcal{b}}} = 4\int_0^{\mathcal{b}_2} \frac{d\mathcal{b}}{\{2[K - \Phi(\mathcal{b})]\}^{\frac{1}{2}}} . \tag{33}$$

Although this solution is a standing wave, $\mathcal{b}$ does not oscillate sinusoidally, so this mode cannot be viewed as a superposition of circularly polarized parallel propagating Alfvén waves.

Case 2. Unstable Plasma

Assume that Eq. (30) does not hold, i.e., assume

$$(p_{\parallel})_{\mathcal{b}=0} > (p_{\perp})_{\mathcal{b}=0} + B_0^2/4\pi . \tag{34}$$

The plasma is unstable with respect to small-amplitude Alfvén waves, and the magnetic potential Φ has the form sketched in Fig. 3(b)-(d). The evolution of the circularly polarized Alfvén wave depends on the value of K relative to $\Phi(0)$.

(a) Assume $K > \Phi(0)$, which corresponds to Fig. 3(b). Let $\Phi(\mathcal{b}_1) = \Phi(\mathcal{b}_2) = K$, where $-\mathcal{b}_1 = \mathcal{b}_2 > 0$ as before.

As in Case 1 for large-amplitude waves, $\mathcal{b}$ oscillates between the values $\mathcal{b}_1$ and $\mathcal{b}_2$ with period τ given by Eq. (33). The oscillation is nonsinusoidal to the extent that Φ is nonparabolic. The development of the magnetic field in time can be seen in Fig. 2: a complete cycle consists of the sequence (a)···(f)(g)(f)···(a); $\mathcal{b}$ passes through zero twice each period.

(b) Assume $K \approx \Phi(0)$, which corresponds to Fig. 3 (c).

The case $K = \Phi(0)$ is the situation usually considered in instability studies: the plasma is unstable, but initially unperturbed. If a small amplitude circularly polarized Alfvén wave perturbation is introduced with $\mathcal{b}(0) > 0$ and $\dot{\mathcal{b}}(0) > 0$, $\mathcal{b}$ initially grows exponentially, then more slowly until its growth stops at $\mathcal{b}_2$, the positive root of $\Phi(\mathcal{b}) = K$. Immediately the mode decays, with $\mathcal{b}$ ultimately falling exponentially to zero.

The time τ required for the amplitude to reach saturation and decay to its initial amplitude $\mathcal{b}(0)$ is

$$\tau = 2 \int_{\mathcal{b}(0)}^{\mathcal{b}_2} \frac{d\mathcal{b}}{\dot{\mathcal{b}}} . \tag{35}$$

The exponential rate for growth and decay is the usual firehose growth rate. The duration of exponential growth will be arbitrarily long as $\mathcal{b}(0)$ is made arbitrarily small, although in practice $\mathcal{b}(0)$ cannot be made much less than the inherent random fluctuations in $\underset{\sim}{B}$.

The growth-decay behavior is demonstrated in Fig. 2 by the sequence (c)(b)(a)(b)(c), with ultimate decay to the uniform magnetic field pictured in Fig. 2(d).

When $K = \Phi(0)$ the exact equations predict pure decay, or growth-saturation-decay, but the mode is not periodic. When K is near $\Phi(0)$, but not equal to it, any circularly polarized wave oscillates between solutions of $\Phi(\mathcal{b}) = K$. The perturbation amplitude spends most of its time near zero amplitude, since $\dot{\mathcal{b}}$ is small there. The period increases markedly as K approaches $\Phi(0)$.

(c) Assume $\Phi_{min} < K < \Phi(0)$, where Φ_{min} denotes the minimum value of $\Phi(\mathcal{b})$, corresponding to Fig. 3(d).

Let $\Phi(\mathcal{b}_1) = \Phi(\mathcal{b}_2) = K$, where $0 < \mathcal{b}_1 < \mathcal{b}_2$, and choose the coordinate system so that $\mathcal{b}_1 \leqslant \mathcal{b}(0) \leqslant \mathcal{b}_2$. Figure 3(d) shows that $\mathcal{b}$ oscillates between the limits $\mathcal{b}_1$ and $\mathcal{b}_2$, never passing through zero. The field behavior for a full cycle is illustrated in Fig. 2 by the sequence (a)(b)(c)(b)(a).

III. PARALLEL ALFVÉN WAVES IN THE GUIDING CENTER MODEL

The results obtained in Sec. II in the CGL model also follow from the Guiding Center equations, which, because the heat-flow tensor is not arbitrarily neglected, constitute a more realistic approximation to an actual plasma. We work with the equations obtained by Kulsrud from the Vlasov equation in the small gyroradius limit.[3] This is a kinetic description, and thus the particle distribution function F_0 must be specified. We take F_0 to be bi-Maxwellian:

$$F_0(w,q,t) = C p_\perp^{-1} p_{||}^{-\frac{1}{2}} \exp[-\rho w/p_\perp - \tfrac{1}{2}\rho(q - u_{||})^2/p_{||}], \tag{36}$$

where

$$w \equiv \tfrac{1}{2}(\underset{\sim}{v} - \underset{\sim}{u})_\perp^{\,2} \tag{37}$$

and

$$q \equiv v_{||} \,. \tag{38}$$

Parallel and perpendicular refer to the total magnetic field.

Using Eq. (36) and the characteristics (9) of the waves of interest, we show in Appendix B that Kulsrud's GC equations reduce to

$$E_{||} = 0, \tag{39}$$

$$\partial \underset{\sim}{b}/\partial t = B_0 \, \partial \underset{\sim}{u}/\partial z, \tag{40}$$

$$\rho \partial \underset{\sim}{u}/\partial t = -(B_0/B^2)(p_\triangle - B^2/4\pi)\partial \underset{\sim}{b}/\partial z, \tag{41}$$

$$p_\perp(t)/p_\perp(0) = B(t)/B(0), \tag{42}$$

$$p_{||}(t)/p_{||}(0) = B^2(0)/B^2(t), \tag{43}$$

$$2\dot{B}/B = \rho(p_\triangle - B^2/4\pi)^{-1} \, \partial u^2/\partial t, \tag{44}$$

$$(\underset{\sim}{u} \cdot \underset{\sim}{b})\dot{B} = 0. \tag{45}$$

Equations (40) through (43) are identical to those obtained from the CGL model, Eqs. (10) through (13). Equation (39) disposes of the parallel electric field, which appears in the GC theory, but not in the CGL model.

A. Constant-Amplitude Solutions in the GC System

The solutions of the CGL system considered in Sec. II A have the property that $|\underset{\sim}{B}|$ and $|\underset{\sim}{u}|$ remain constant in time. Thus both sides of Eq. (44) vanish, Eq. (45) is satisfied, and the GC equations reduce to those derived from the CGL model and lead to the same solutions as obtained in Sec. II A.

B. Time-Varying-Amplitude Solutions in the GC System

The time-varying-amplitude Alfvén modes considered in Sec. II B satisfy Eq. (44) in view of Eq. (27) and a simple manipulation of Eq. (22). Equation (45) is likewise satisfied because Eqs. (23) and (27) show that $\underset{\sim}{b}$ and $\underset{\sim}{u}$ are orthogonal.

The GC equations have thus been simplifed to the CGL results, Eqs. (10) through (13), and lead to the same time-varying-amplitude solutions obtained in Sec. II B.

Note that, since the solutions obtained from the GC equations have a bi-Maxwellian velocity distribution, the heat-flow tensor $\underset{\approx}{Q}$ vanishes. This justifies, in retrospect, the use of the CGL model, which arbitrarily assumes that $\nabla \cdot \underset{\approx}{Q} = 0$.[1,3]

IV. DISCUSSION

A. Significance of the Constant Amplitude Alfvén Wave

It has been known for many years that in a uniform MHD plasma a transverse magnetic perturbation of arbitrary orientation and constant amplitude (or special cases of this type of wave) propagates at the Alfvén velocity parallel to a uniform magnetic field without distortion, i.e., there is no coupling to particles or waves in the absence of other perturbations.[9-12] Sections II A and III A show that this conclusion holds even for an anisotropic plasma in the CGL and GC models. Examples are pictured in Fig. 1.

The constant-amplitude Alfvén wave may be important in the solar wind. Mariner V data[13] show the high correlation or anticorrelation between magnetic field and fluid velocity which characterizes Alfvén waves [see Eq. (18)]. Although the individual field components fluctuate in a seemingly random fashion, the total field magnitude is relatively constant over large regions of the solar wind. The mode propagates at the Alfvén velocity, always away from the sun. Furthermore, the amplitude of the magnetic fluctuation is comparable to the total field, so that explanation of the phenomenon requires a large-amplitude theory. Subsequent analysis of the data may show that the random fluctuations in the observed field can be duplicated by the constant-amplitude Alfvén wave with suitable choice of the arbitrary function Θ. The constant-amplitude Alfvén wave is characterized by a constant magnetic field component B_0 in the direction of propagation; it has not been determined whether the solar wind has this property.[14]

The simple picture of a constant-amplitude wave propagating parallel to the uniform field without distortion may no longer be valid if other waves are present. It has been shown, for example, that a large-amplitude circularly polarized Alfvén wave in an MHD plasma ($p_{\parallel} = p_{\perp}$) can couple to another Alfvén wave and an ion sound wave if the waves satisfy certain three-wave resonance conditions.[9]

B. The Variable-Amplitude Circularly Polarized Alfvén Mode

Earlier quasilinear studies[4-6] of the firehose mode produced equations accurate to second order in the wave amplitudes of the form

$$d\langle P_{\perp}\rangle/dt = (\langle P_{\parallel}\rangle/B_0^{\,2}) \int d^3k\ \gamma(\underset{\sim}{k},t)\psi(\underset{\sim}{k},t), \tag{46}$$

$$d\langle P_{\parallel}\rangle/dt = [(4\langle P_{\parallel}\rangle - 2\langle P_{\perp}\rangle)/B_0^{\,2}] \int d^3k\ \gamma(\underset{\sim}{k},t)\ \psi(\underset{\sim}{k},t), \tag{47}$$

$$d\psi(\underset{\sim}{k},t)/dt = 2\gamma(\underset{\sim}{k},t)\ \psi(\underset{\sim}{k},t), \tag{48}$$

$$\gamma^2(\underset{\sim}{k},t) = \rho^{-1}(\underset{\sim}{k}\cdot\hat{B}_0)^2(\langle P_{\parallel}\rangle - \langle P_{\perp}\rangle - B_0^{\,2}/4\pi), \tag{49}$$

$$\psi(\underset{\sim}{k},t)\ \delta(\underset{\sim}{k} + \underset{\sim}{k}') \equiv \langle \delta\underset{\sim}{B}(\underset{\sim}{k},t)\cdot\delta\underset{\sim}{B}(\underset{\sim}{k}',t)\rangle. \tag{50}$$

Here $\delta\underset{\sim}{B}$ is the perturbation in the magnetic field, parallel and perpendicular refer to the direction of $\underset{\sim}{B}_0$, and finite gyroradius effects have been dropped. The brackets denote ensemble and spatial averaging in the derivation of Davidson and Völk. Equations (46) through (50) are obtained in Appendix A from the CGL model without the necessity of taking ensemble averages.

The quasilinear equations have the advantage of treating an arbitrary distribution of linearly polarized Alfvén waves. They imply

the existence of a quenching point: the plasma is initially unstable if $\langle P_{\parallel}\rangle(0) > \langle P_{\perp}\rangle(0) + B_0^2/4\pi$, but, as the waves grow, $\langle P_{\perp}\rangle$ increases and $\langle P_{\parallel}\rangle$ decreases until $\gamma(\underset{\sim}{k},t) = 0$, and no waves are unstable.

However, Eqs. (46) through (50) have not been solved in even the simplest cases. The qualitative properties of the quenching process obtained so simply in Sec. II B for the circularly polarized mode--namely, that quenching occurs in a finite time and is followed immediately by decay--are obscured by the complexity of Eqs. (46) through (50). Indeed these gross features may have been lost by the approximations used in deriving them from the more fundamental equations. The quasi-linear theory cannot provide quantitative information concerning the quenching process, since, as Davidson and Völk note, higher-order nonlinear effects become important as $\gamma \to 0$. In deriving the quasi-linear equations one treats $\gamma^2(\underset{\sim}{k},t)$ as a zero-order quantity, an assumption which clearly breaks down at the quenching point.

Qualitative features of the quenching of the circularly polarized Alfvén wave are shared by other wave saturation processes:

1. Numerical studies of the flute mode in the low-density regime show exponential growth at small amplitudes, then saturation followed by decay.[15] The energy in the mode oscillates, much like the Alfvén wave of Case 2 (b), Sec. II B, when K is slightly less than $\Phi(0)$.

2. Investigation of the nonlinear evolution of a single-wavelength longitudinal flute mode with frequency near a harmonic of the gyrofrequency in a loss-cone plasma indicates saturation in a finite

time followed by decay.[16] The analysis is invalid beyond the decay regime, so that oscillatory behavior cannot be revealed. The mode considered is a symmetric standing wave, and the analysis involves a pseudopotential, both characteristics having analogues in the theory of Sec. II B.

3. In a plasma consisting of two cold streams, a dynamical theory of the two-stream instability shows that "the electric field does not grow and level off at some value E_{max} where $\gamma = 0$, but, rather, because of the dynamics, overshoots this point and then oscillates back to its initial state."[17]

4. The bump-on-the-tail limit of the two-stream instability has similar properties: wave saturation occurs in a finite time and is followed by gentle oscillations of the wave energy, with period comparable to particle-trapping times.[18-20]

C. Conclusion

No pretense is made that all the special modes discussed here are significant in the physical world. The requirement of a uniform infinite plasma in a uniform magnetic field subject to no perturbation except the modes of interest is enough to preclude their occurrence. It is hoped that the advantage of having an exact solution in a simple form to an otherwise intractable class of problems will make this study beneficial. The characteristics of the simple wave-quenching process may serve a useful purpose if only pointing the way to important characteristics of more complete and more complex plasma instability problems.

ACKNOWLEDGMENTS

The author is indebted to Allan N. Kaufman for guidance, criticism, and encouragement during the course of this research.

APPENDIX A. QUASILINEAR THEORY OF THE FIREHOSE INSTABILITY IN THE CGL MODEL

We outline a derivation from the CGL equations of the quasilinear results obtained by Davidson and Völk.[4] It is not surprising that identical results follow, because the assumption of diagonal pressure tensor and neglect of the heat-flow tensor explicit in their work are used in deriving the CGL equations. It is useful, however, to point out an important difference between the definition of the average pressures in the two analyses. Note, also, that in our analysis the ensemble averages used by Davidson and Völk are never required: it suffices to consider only spatially averaged quantities.

We assume a uniform, infinitesimally perturbed plasma in a uniform magnetic field $\underset{\sim}{B}_0$. We view all CGL variables as consisting of a space-average part, which may depend on time, and a fluctuating part: $\rho(\underset{\sim}{x},t) = \langle\rho\rangle(t) + \delta\rho(\underset{\sim}{x},t)$, etc. The hexagonal brackets denote spatial averaging.

Taking the space-average of the CGL Eqs. (1) through (3), we find

$$\langle\rho\rangle(t) = \text{constant} = \rho, \tag{A.1}$$

$$\langle\underset{\sim}{u}\rangle(t) = \text{constant} = 0, \tag{A.2}$$

$$\langle\underset{\sim}{B}\rangle(t) = \text{constant} = \underset{\sim}{B}_0. \tag{A.3}$$

When the CGL Eqs. (1) through (8) are linearized in fluctuations about these spatial averages and the unstable Alfvén wave characteristics

are assumed, the usual linearly polarized firehose waves follow. To first order in the perturbation we find

$$\delta\rho = 0, \tag{A.4}$$

$$p_\perp = \langle p_\perp \rangle(t), \tag{A.5}$$

$$p_{||} = \langle p_{||} \rangle(t), \tag{A.6}$$

$$\delta \underset{\sim}{B}(\underset{\sim}{k},t) = \delta \underset{\sim}{B}(\underset{\sim}{k},0)\, e^{\gamma(\underset{\sim}{k},t)t}, \tag{A.7}$$

$$\delta \underset{\sim}{u}(\underset{\sim}{k},t) = -i\, \gamma(\underset{\sim}{k},t)(\underset{\sim}{k}\cdot\underset{\sim}{B}_0)^{-1}\, \delta \underset{\sim}{B}(\underset{\sim}{k},t), \tag{A.8}$$

$$\gamma(\underset{\sim}{k},t) = \pm(\underset{\sim}{k}\cdot\hat{B}_0)[(\langle p_\Delta \rangle(t) - B_0{}^2/4\pi)/\rho]^{-\frac{1}{2}} . \tag{A.9}$$

We assume that the firehose instability criterion holds so that the growth rate $\gamma(\underset{\sim}{k},t)$ is real. The field fluctuation $\delta \underset{\sim}{B}$ is perpendicular to $\underset{\sim}{k}$ and $\underset{\sim}{B}_0$, a characteristic of Alfvén waves.

The average pressures are constant to first order; to calculate their second-order evolution in time it suffices to carry the two adiabatic equations (4) and (5) to second order in the perturbation and space average the result. We find

$$\partial\langle p_\perp \rangle/\partial t = (\langle p_\perp \rangle/B_0{}^2) \int d^3k\, \gamma(\underset{\sim}{k},t)\, \psi(\underset{\sim}{k},t), \tag{A.10}$$

$$\partial\langle p_{||} \rangle/\partial t = -2(\langle p_{||} \rangle/B_0{}^2) \int d^3k\, \gamma(\underset{\sim}{k},t)\, \psi(\underset{\sim}{k},t), \tag{A.11}$$

where the magnetic field spectral density ψ is defined by

$$\psi(\underset{\sim}{k},t)\, \delta(\underset{\sim}{k} + \underset{\sim}{k}') \equiv \langle \delta \underset{\sim}{B}(\underset{\sim}{k},t)\cdot\delta \underset{\sim}{B}(\underset{\sim}{k}',t) \rangle \tag{A.12}$$

and satisfies

$$\partial\psi(\underset{\sim}{k},t)/\partial t = 2\gamma(\underset{\sim}{k},t)\,\psi(\underset{\sim}{k},t) \,. \tag{A.13}$$

In order to compare the results (A.10) through (A.13) with those of Davidson and Völk, we note that $p_\perp$, which appears in the CGL equations, is the pressure perpendicular to the local magnetic field $\underset{\sim}{B} = \underset{\sim}{B}_0 + \delta\underset{\sim}{B}$, whereas the quantity $P_\perp$, which is used in the earlier work, is the pressure perpendicular to $\underset{\sim}{B}_0$. Similar remarks apply to $p_{||}$ and $P_{||}$. Thus we have

$$\langle p_{||}\rangle \equiv \langle \underset{\approx}{p} : \hat{B}\hat{B}\rangle, \tag{A.14}$$

$$\langle p_\perp\rangle \equiv \langle \underset{\approx}{p} : (\underset{\approx}{I} - \hat{B}\hat{B})\rangle, \tag{A.15}$$

$$\langle P_{||}\rangle \equiv \langle \underset{\approx}{p} : \hat{B}_0\hat{B}_0\rangle, \tag{A.16}$$

$$\langle P_\perp\rangle \equiv \langle \underset{\approx}{p} : (\underset{\approx}{I} - \hat{B}_0\hat{B}_0)\rangle. \tag{A.17}$$

To second order it follows that

$$\langle P_\perp\rangle = \langle p_\perp\rangle + (\langle p_\Delta\rangle/2B_0^{\,2}) \int d^3k\, \psi(\underset{\sim}{k},t), \tag{A.18}$$

$$\langle P_{||}\rangle = \langle p_{||}\rangle - (\langle p_\Delta\rangle/B_0^{\,2}) \int d^3k\, \psi(\underset{\sim}{k},t). \tag{A.19}$$

Note that $\langle p_\perp\rangle - \langle P_\perp\rangle$ is a second-order quantity, and similarly for $\langle p_{||}\rangle - \langle P_{||}\rangle$. Thus to the required accuracy, $\langle p_\Delta\rangle(t)$ in Eq. (A.9) may be replaced by $\langle P_\Delta\rangle(t)$.[21]

Taking the time derivative of (A.18) and (A.19), we have

$$\partial\langle P_{\perp}\rangle/\partial t = (\langle P_{||}\rangle/B_0^{\,2}) \int d^3k\ \gamma(\underset{\sim}{k},t)\ \psi(\underset{\sim}{k},t), \tag{A.20}$$

$$\partial\langle P_{||}\rangle/\partial t = -[(4\langle P_{||}\rangle - 2\langle P_{\perp}\rangle)/B_0^{\,2}] \int d^3k\ \gamma(\underset{\sim}{k},t)\ \psi(\underset{\sim}{k},t). \tag{A.21}$$

Equations (A.9), (A.12), (A.13), (A.20), and (A.21) are identical to Eqs. (46) through (50) obtained by Davidson and Völk. Finite gyroradius effects have been ignored here and should be included in a more complete treatment.

APPENDIX B. GUIDING CENTER EQUATIONS FOR THE PARALLEL ALFVÉN WAVE

We start with the guiding-center equations in the form obtained by Kulsrud.[3] This system, which Kulsrud terms the "Adiabatic Equations," is

$$\partial\rho/\partial t + \nabla\cdot(\rho\underset{\sim}{u}) = 0, \tag{B.1}$$

$$\rho d\underset{\sim}{u}/dt = -\nabla\cdot\underset{\approx}{p} + (\nabla \times \underset{\sim}{B}) \times \underset{\sim}{B}/4\pi, \tag{B.2}$$

$$\underset{\approx}{p} = p_{||}\,\hat{B}\hat{B} + p_{\perp}(\underset{\approx}{I} - \hat{B}\hat{B}), \tag{B.3}$$

$$p_{||} = \sum m \int F_0 (q - u_{||})^2\, 2\pi\, dq\, dw, \tag{B.4}$$

$$p_{\perp} = \sum m \int F_0\, w\, 2\pi\, dq\, dw, \tag{B.5}$$

$$\partial F_0/\partial t + (\underset{\sim}{\alpha} + q\hat{B})\cdot\nabla F_0 + wW\partial F_0/\partial w + Q\partial F_0/\partial q = 0, \tag{B.6}$$

$$W \equiv \hat{B}\hat{B} : \nabla\underset{\sim}{\alpha} - \nabla\cdot\underset{\sim}{\alpha} - q\nabla\cdot\hat{B}, \tag{B.7}$$

$$Q \equiv \underset{\sim}{\alpha}\cdot\partial\hat{B}/\partial t + \underset{\sim}{\alpha}\underset{\sim}{\alpha} : \nabla\hat{B} + q\underset{\sim}{\alpha}\hat{B} : \nabla\hat{B} + w\nabla\cdot\hat{B} + eE_{||}/m, \tag{B.8}$$

$$\underset{\sim}{\alpha} \equiv \underset{\sim}{u} - \underset{\sim}{u}\cdot\hat{B}\hat{B}, \tag{B.9}$$

$$\nabla\cdot\underset{\sim}{B} = 0, \tag{B.10}$$

$$\partial\underset{\sim}{B}/\partial t = \nabla \times (\underset{\sim}{u} \times \underset{\sim}{B}), \tag{B.11}$$

$$\sum e \int F_0\, dq\, dw = 0, \tag{B.12}$$

$$\sum e \int F_0\, q\, dq\, dw = 0, \tag{B.13}$$

$$E_{\parallel} = \sum (e/m)\, \hat{B}\cdot(\nabla\cdot\underset{\sim}{p})/(\sum N\, e^2/m), \tag{B.14}$$

$$w \equiv (\underset{\sim}{v} - \underset{\sim}{u})_{\perp}^{2}, \tag{B.15}$$

$$q = v_{\parallel}. \tag{B.16}$$

In these equations the notation of the CGL model, Eqs. (1) through (8), has been used where applicable; the particle distribution function F_0 depends on the particle velocity $\underset{\sim}{v}$ through q and w; parallel and perpendicular refer to the direction of the local magnetic field $\underset{\sim}{B}$; $E_{\parallel}$ is the parallel electric field component; and the summations in Eqs. (B.4) through (B.14) are over particle species.

It is convenient to simplify Eqs. (B.7) and (B.8) by using (B.9) to eliminate $\underset{\sim}{\alpha}$ in favor of the fluid velocity $\underset{\sim}{u}$. We find

$$W = \hat{B}\hat{B} : \nabla\underset{\sim}{u} - \nabla\cdot\underset{\sim}{u} - q\nabla\cdot\hat{B}, \tag{B.17}$$

$$Q = \underset{\sim}{u}\cdot\partial\hat{B}/\partial t + [\underset{\sim}{u}\underset{\sim}{u} + (q - \underset{\sim}{u}\cdot\hat{B})\underset{\sim}{u}\hat{B}] : \nabla\hat{B} + w\nabla\cdot\hat{B} + eE_{\parallel}/m. \tag{B.18}$$

We consider Alfvén waves having properties (3) and use these characteristics to simplify (B.1) through (B.18).

Equations (B.1) and (B.10) are trivially satisfied.

Equations (B.2) and (B.3) reduce to

$$\rho\partial\underset{\sim}{u}/\partial t = -[p_{\Delta} - B^2/4\pi]\, B^{-2}\, B_0 \partial\underset{\sim}{b}/\partial z. \tag{B.19}$$

Equation (B.11) becomes

$$\partial\underset{\sim}{b}/\partial t = B_0\, \partial\underset{\sim}{u}/\partial z. \tag{B.20}$$

The wave equation (14) is readily obtained from (B.19) and (B.20).

Equation (B.14) gives

$$E_{\parallel} = 0. \tag{B.21}$$

Finally, Eqs. (B.17) and (B.18) simplify to

$$W = \frac{1}{2} B^{-2} \partial B^2/\partial t = \dot{B}/B \tag{B.22}$$

and

$$Q = -(\underset{\sim}{u}\cdot\underset{\sim}{b}\ \dot{B}/B^2) - \frac{1}{2}\rho(q - \underset{\sim}{u}\cdot\hat{B})(p_{\Delta} - B^2/4\pi)^{-1}\ \partial u^2/\partial t. \tag{B.23}$$

We assume a bi-Maxwellian distribution function:

$$F_0(w,q,t) = C\ p_{\perp}^{-1}\ p_{\parallel}^{-\frac{1}{2}} \exp[-\rho w/p_{\perp} - \rho(q - u_{\parallel})^2/2p_{\parallel}]. \tag{B.24}$$

The appropriate time dependence of the normalization factor is included in Eq. (B.24). With this choice, Eqs. (B.4) and (B.5) give the appropriate pressures. The quasineutrality condition (B.12) holds for all times if it is true initially, and Eq. (B.13) requires that the fluid velocity be the same for electrons and ions, $u_{\parallel}^{e} = u_{\parallel}^{i}$. Equations (B.6), (B.22), (B.23), and (B.24) reduce to

$$\{-\dot{p}_{\perp}/p_{\perp} - \frac{1}{2}\dot{p}_{\parallel}/p_{\parallel} + \rho w\dot{p}_{\perp}/p_{\perp}^{2} + \frac{1}{2}\rho(q - u_{\parallel})^2\ \dot{p}_{\parallel}/p_{\parallel}^{2} - w(\dot{B}/B)\rho/p_{\perp}$$
$$+ [(\underset{\sim}{u}\cdot\underset{\sim}{b})\dot{B}/B^2 + \frac{1}{2}\rho(q - u_{\parallel})(p_{\Delta} - B^2/4\pi)^{-1}\ \partial u^2/\partial t]\ \rho(q - u_{\parallel})/p_{\parallel}\}F_0 = 0. \tag{B.25}$$

Since F_0 is never zero, and since $(q - u_{\parallel})$ and w are independent variables, the coefficients of w, 1, $(q - u_{\parallel})$, and $(q - u_{\parallel})^2$ in the curly brace of Eq. (B.25) must vanish:

$$\dot{p}_\perp/p_\perp - \dot{B}/B = 0, \tag{B.26}$$

$$\dot{p}_\perp/p_\perp + \frac{1}{2}\dot{p}_\parallel/p_\parallel = 0, \tag{B.27}$$

$$(\underset{\sim}{u}\cdot\underset{\sim}{b})\dot{B} = 0, \tag{B.28}$$

$$\dot{p}_\parallel/p_\parallel + \rho(p_\Delta - B^2/4\pi)^{-1}\,\partial u^2/\partial t = 0. \tag{B.29}$$

Equations (B.26) and (B.27) give

$$p_\perp(t)/p_\perp(0) = B(t)/B(0) \tag{B.30}$$

and

$$p_\parallel(t)/p_\parallel(0) = B^2(0)/B^2(t). \tag{B.31}$$

Thus for the Alfvén modes under consideration and for a bi-Maxwellian particle distribution, the GC equations reduce to Eqs. (B.19) through (B.21) and (B.28) through (B.31). Equations (39) through (43) and (45) are equivalent to Eqs. (B.21), (B.20), (B.19), (B.30), (B.31), and (B.28), respectively. Equation (44) follows from Eq. (B.29) when $\dot{p}_\parallel$ is eliminated by means of Eq. (B.31).

FOOTNOTES AND REFERENCES

* This work was supported by the U. S. Atomic Energy Commission and NASA.

1. G. F. Chew, M. L. Goldberger, and F. E. Low, Proc. Roy. Soc. (London) A236, 112 (1956).
2. Harold Grad, Proc. Symp. Appl. Math. 18, 162 (1967).
3. Russell Kulsrud, General Stability Theory in Plasma Physics, Advanced Plasma Theory, Course 25, Edited by M. N. Rosenbluth (Academic Press, New York and London, 1964).
4. R. C. Davidson and H. J. Völk, Phys. Fluids 11, 2259 (1968).
5. V. D. Shapiro and V. I. Shevchenko, Zh. Eksperim. i Teor. Fiz. (USSR) 45, 1612 (1963) [English translation: Soviet Physics-JETP 18, 1109 (1964)].
6. Aaron Barnes, Phys. Fluids 11, 2644 (1968).
7. I. A. Akhiezer, R. V. Polovin and N. L. Tsintsadze, Zh. Eksperim. i Teor. Fiz. (USSR) 37, 756 (1959) [English translation: Soviet Physics-JETP 37(10), 539 (1960)].
8. It is possible to find nontrivial Alfvén waves with properties (9a)-(9h) because there exist plane polarized Alfvén modes propagating parallel to $\underset{\sim}{B}_0$ with polarization planes orthogonal to each other. The suitably phased sum of such waves is a circularly polarized Alvén mode with the property (9e) that the magnitude of the perturbation is constant everywhere. Equation (9e) greatly simplifies the CGL and GC equations. For propagation at an angle to $\underset{\sim}{B}_0$ there is only one Alfvén mode, and the simplifications so useful in the present work cannot occur.

9. R. Z. Sagdeev and A. A. Galeev, Nonlinear Plasma Theory, Edited by T. M. O'Neil and D. L. Book (W. A. Benjamin, Inc., Amsterdam, 1969).

10. V. C. A. Ferraro, Proc. Roy Soc. (London) A233, 310 (1956).

11. A. A. Vedenov, E. P. Velikhov, and R. Z. Sagdeev, Nucl. Fusion 1, 82 (1961).

12. A. A. Galeev and V. N. Oraevskii, Dokl. Akad. Nauk. SSSR 154, 1069 (1964) [English translation: Soviet Physics - Doklady 9, 154 (1964)].

13. J. W. Belcher, Leverett Davis, Jr., and E. J. Smith, J. Geophys. Res. 74, 2302 (1969).

14. John Belcher (Calif. Inst. of Technology), private communication, 1970.

15. J. A. Byers, Phys. Fluid 10, 2235 (1967).

16. R. E. Aamodt and S. E. Bodner, Phys. Fluids 12, 1471 (1969).

17. J. P. Friedberg and T. P. Armstrong, Phys. Fluids 11, 2669 (1968).

18. T. P. Armstrong and David Montgomery, Phys. Fluids 12, 2094 (1969).

19. David Mongomery (University of Iowa), private communication, 1970.

20. J. M. Dawson and R. Shanny, Phys. Fluids 11, 1506 (1968).

21. In deriving the relations (A.4) - (A.9) from the linearized equations, we treated γ^2 as a zero order quantity. Carrying the pressure terms in γ^2 to second order is admittedly of questionable value, since other terms of this order have been ignored.

FIGURE CAPTIONS

Fig. 1. Magnetic field lines of the constant-amplitude Alfvén wave for various choices of the function $\Theta(\cdot)$, which specifies the direction of the field disturbance $\underset{\sim}{b}$: (a) $\Theta(x) = \pi \tanh kx$; (b) $\Theta(x) = (\pi/2) \tanh kx$; (c) $\Theta(x) = (7\pi/2) \exp[-(kx)^2]$. In each illustration the field lines make a 45 deg angle with $\underset{\sim}{B}_0$ everywhere, corresponding to $|\underset{\sim}{b}| = B_0$. In (a) and (c) the nearly uniform field at large positive values of $k(z - Vt)$ is parallel to the field at large negative values of $k(z - Vt)$; the exaggerated perspective makes them seem nonparallel.

In the CGL and GC models these field configurations propagate without distortion at the generalized Alfvén velocity V, parallel to $\underset{\sim}{B}_0$.

Fig. 2. Temporal evolution of the time-varying-amplitude Alfvén mode. Field lines are pictured for: (a) $\mathcal{b} \approx 6B_0$, (b) $\mathcal{b} \approx 3B_0$, (c) $\mathcal{b} \approx B_0$, (d) $\mathcal{b} = 0$, (e) $\mathcal{b} \approx -B_0$, (f) $\mathcal{b} \approx -3B_0$, (g) $\mathcal{b} \approx -6B_0$. The helical standing-wave structure is generated by a magnetic field component perpendicular to the uniform field $\underset{\sim}{B}_0$ having signed amplitude $\mathcal{b}(t)$, whose time dependence readily follows from Eqs. (24) and (25). This mode is an exact solution for a stable or unstable plasma in the CGL and GC models.

Fig. 3. Sketch of the magnetic potential $\Phi(\mathcal{b})$, Eq. (25), for the variable-amplitude Alfvén mode with various choices of the plasma parameters: (a) stable plasma with $K > \Phi(0)$, corresponding to Case 1; (b) unstable plasma with $K > \Phi(0)$,

corresponding to Case 2(a); (c) unstable plasma with $K = \Phi(0)$, corresponding to Case 2(b); (d) unstable plasma with $\Phi_{min} < K < \Phi(0)$, corresponding to Case 2(c). In (a), Φ is sketched for the pressure anisotropy $(p_\perp)_{\xi=0} = B_0^2/8\pi$, $(p_\parallel)_{\xi=0} = B_0^2/4\pi$. The unstable plasma in (b)-(d) corresponds to $(p_\perp)_{\xi=0} = B_0^2/4\pi$, $(p_\parallel)_{\xi=0} = 4B_0^2/\pi$. By Eq. (24), the time dependence of the signed amplitude ξ, which determines the evolution of the helical structure pictured in Fig. 2, is the displacement of a unit mass particle of energy K moving in the potential $\Phi(\xi)$.

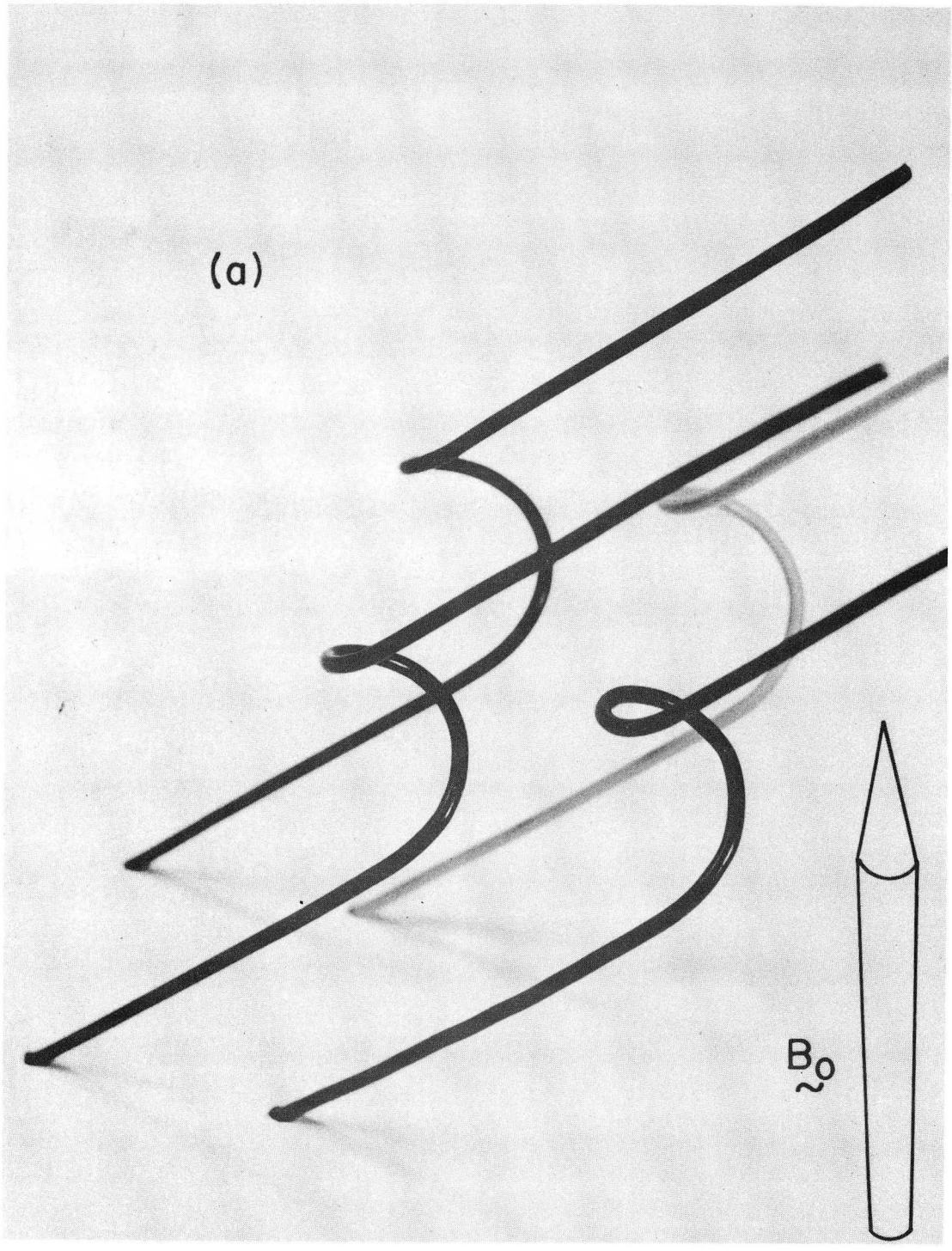

XBB 708-3609A

Fig. 1a

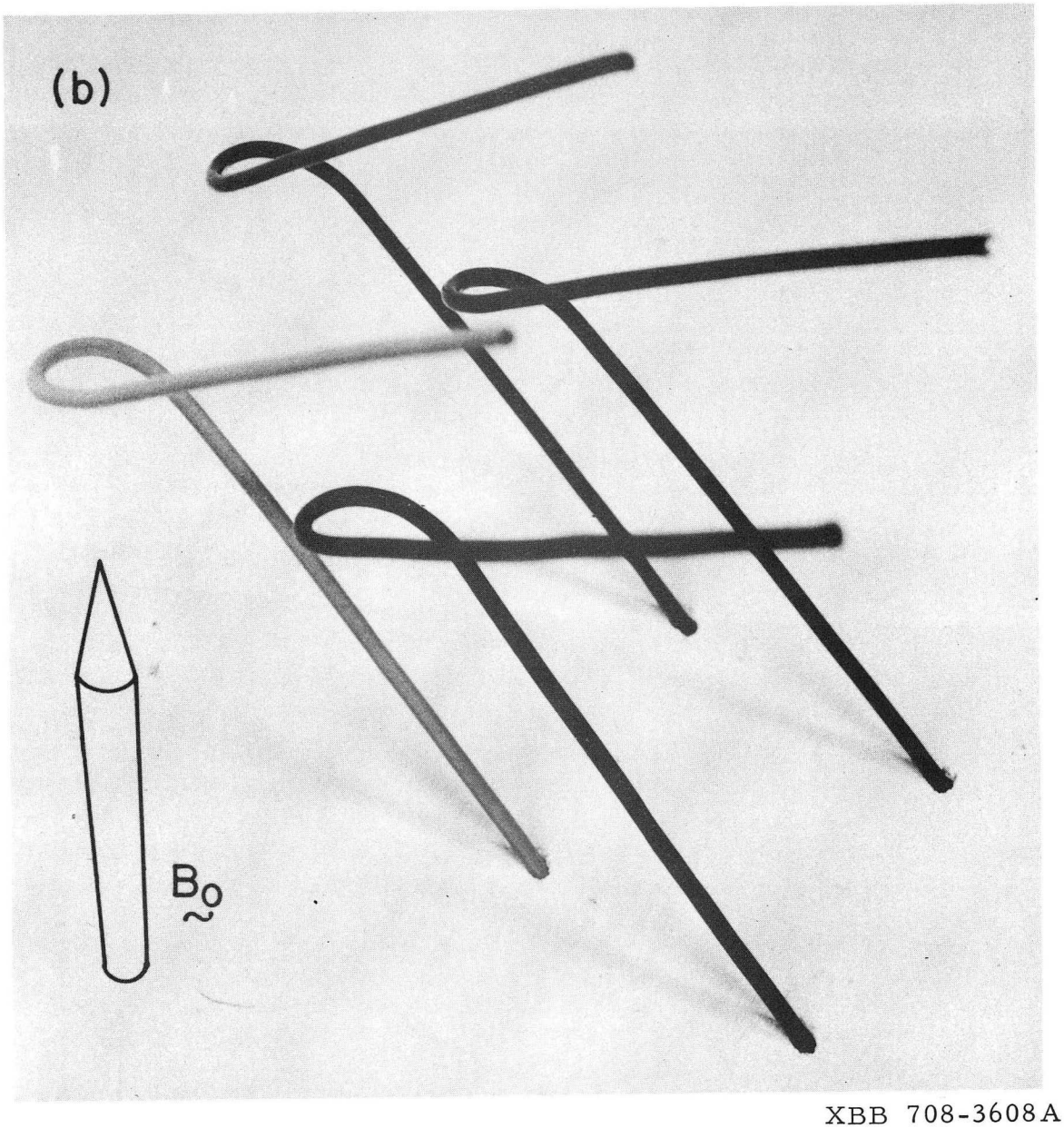

XBB 708-3608A

Fig. 1b

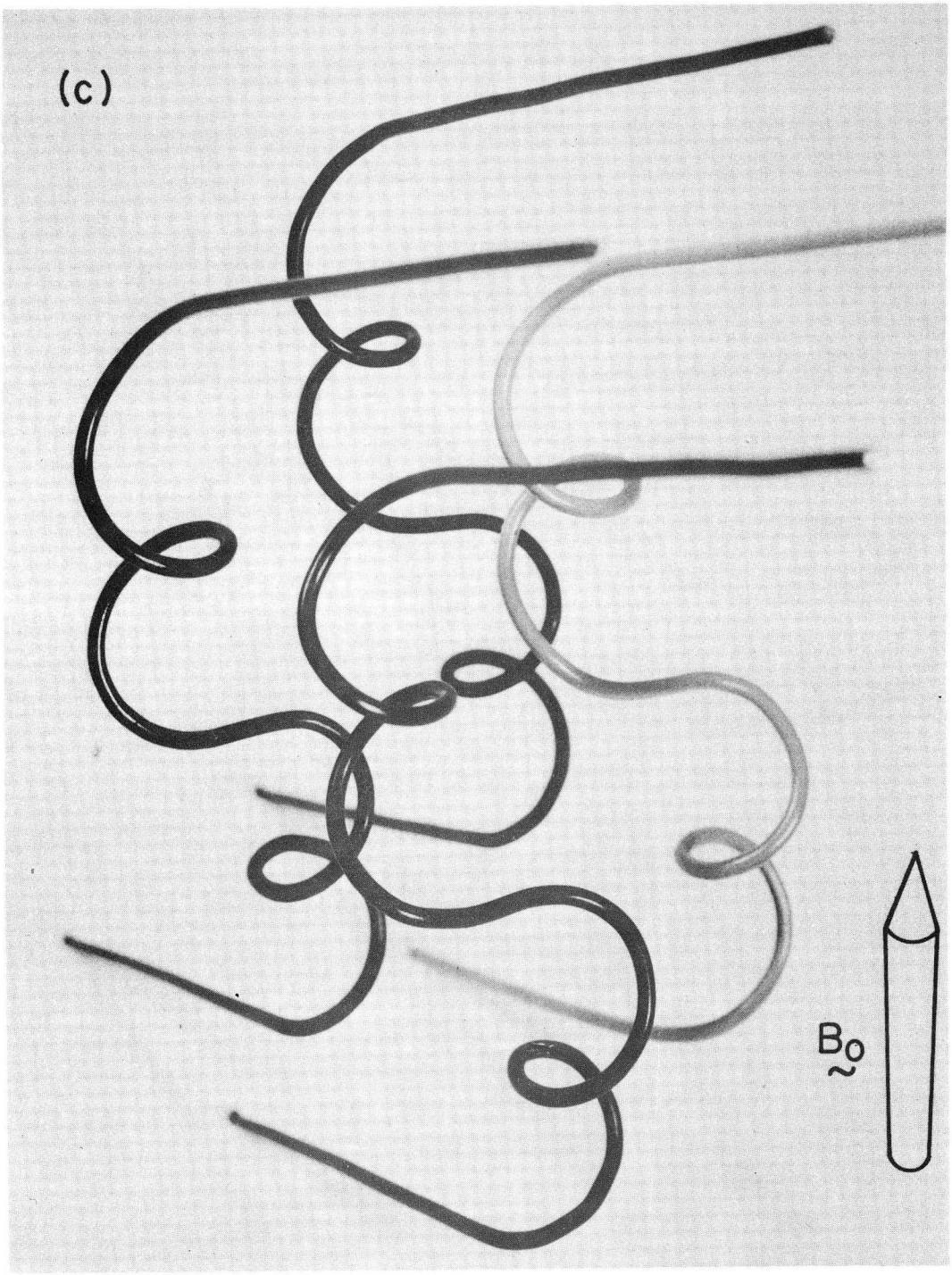

XBB 708-3607A

Fig. 1c

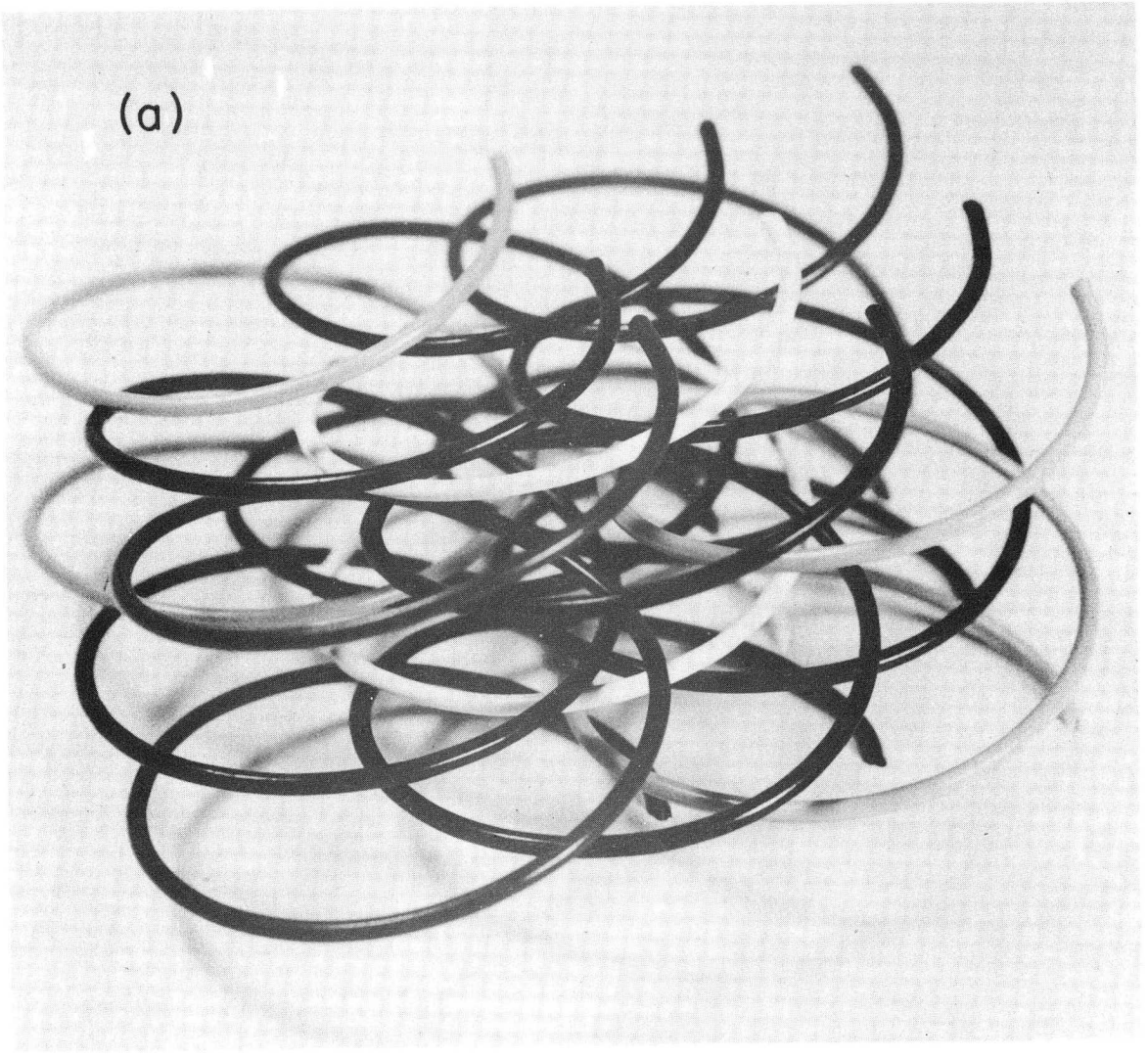

XBB 708-3614A

Fig. 2a

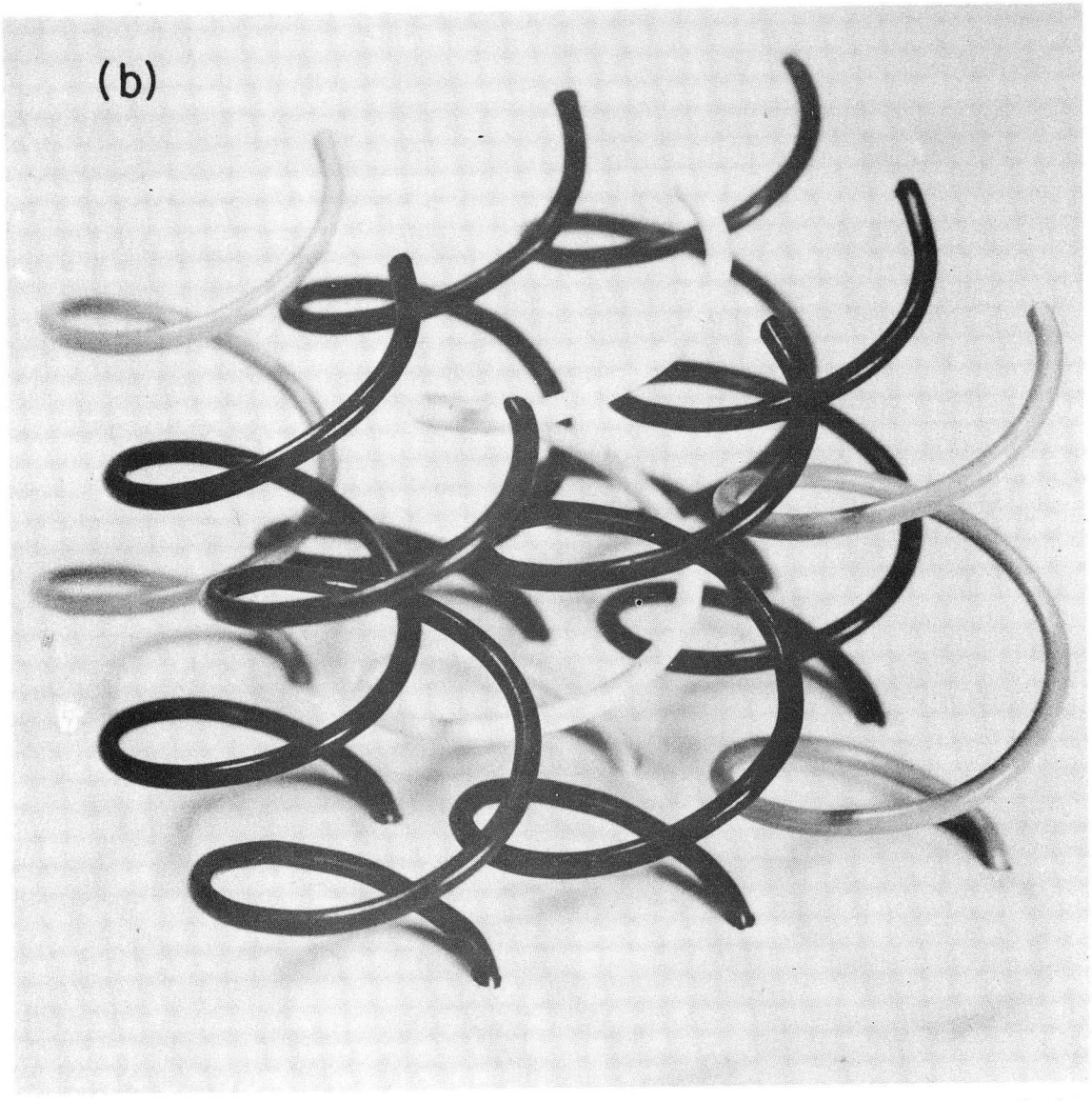

XBB 708-3616A

Fig. 2b

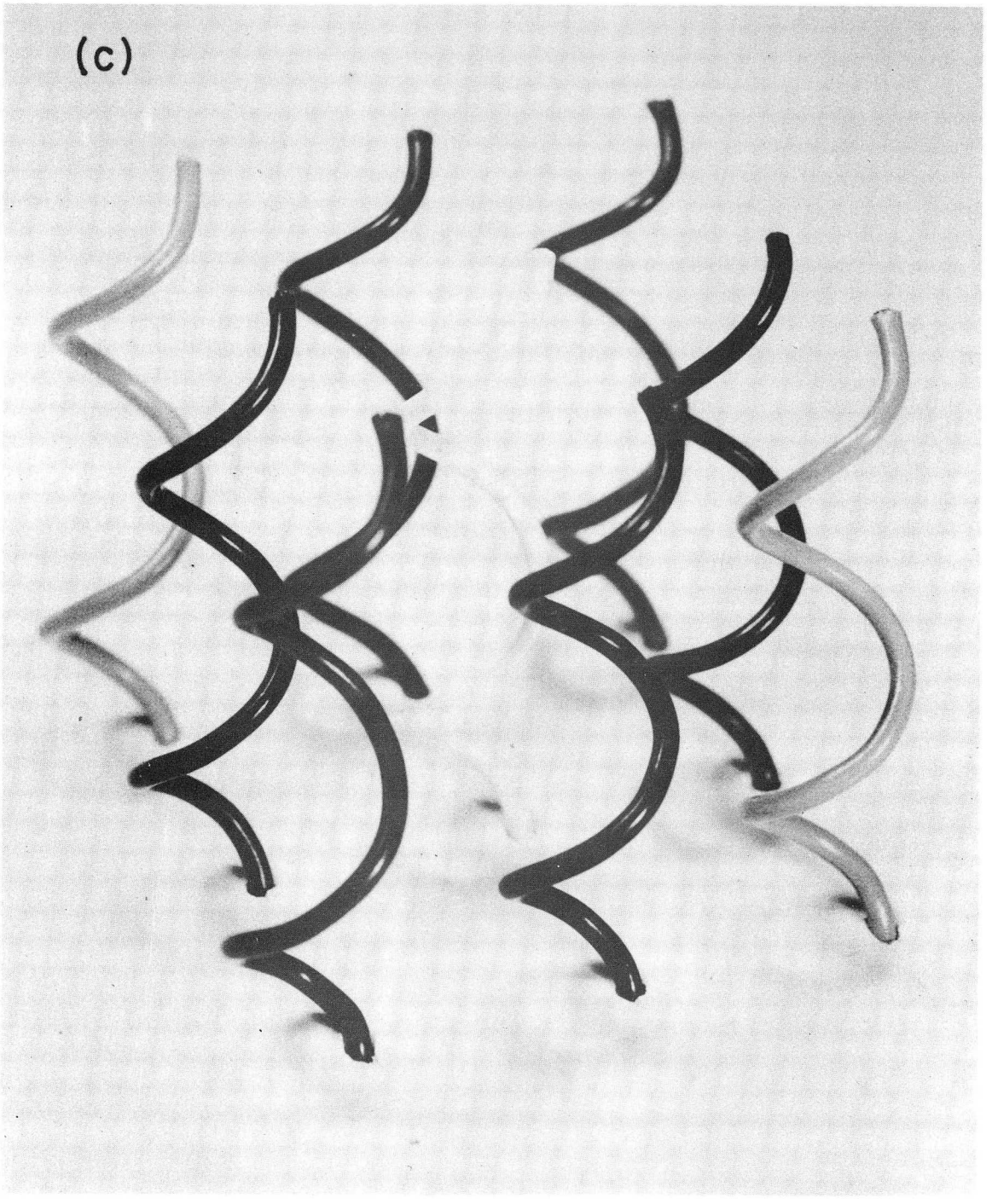

XBB 708-3611A

Fig. 2c

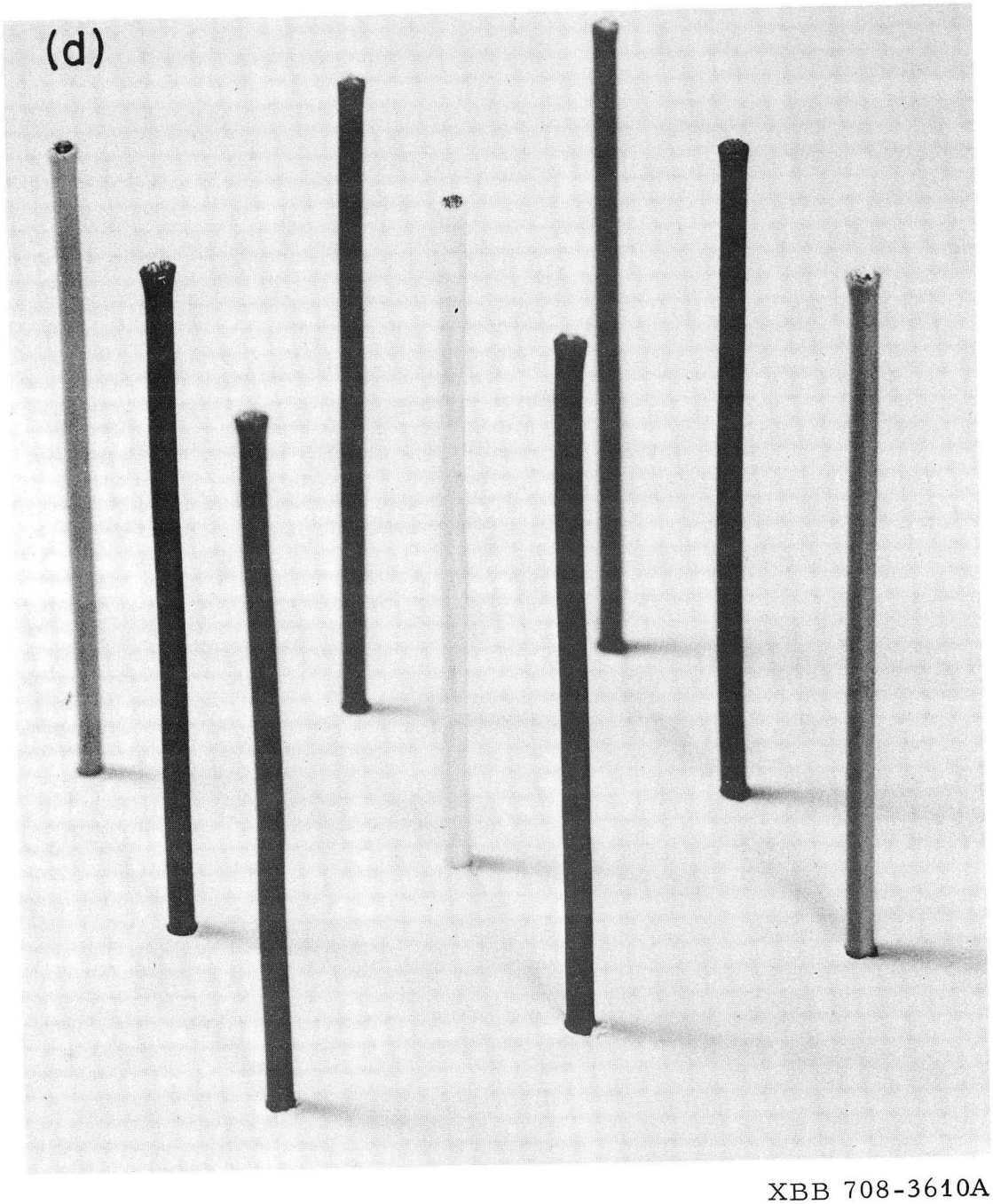

XBB 708-3610A

Fig. 2d

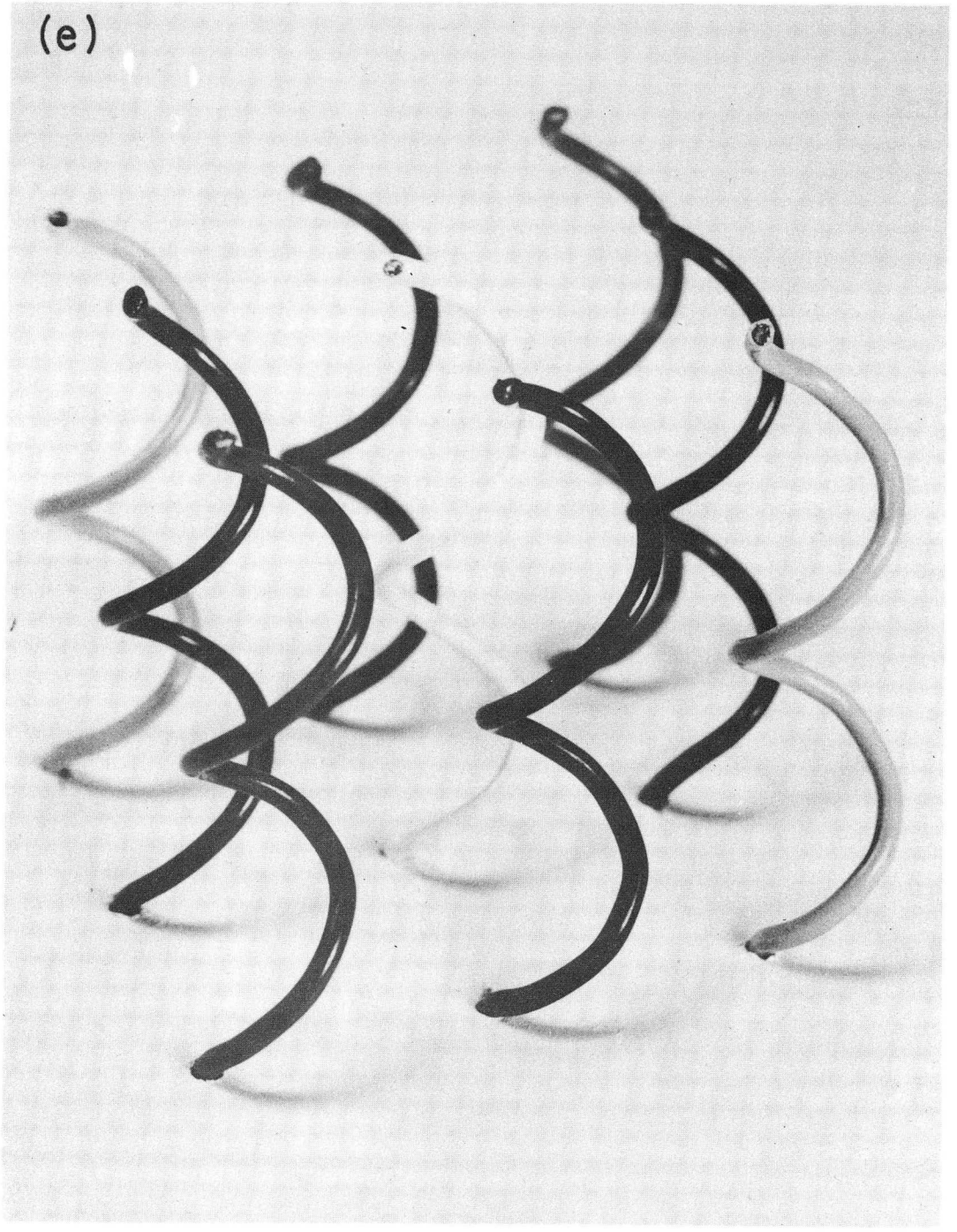

XBB 708-3612A

Fig. 2e

XBB 708-3615A

Fig. 2f

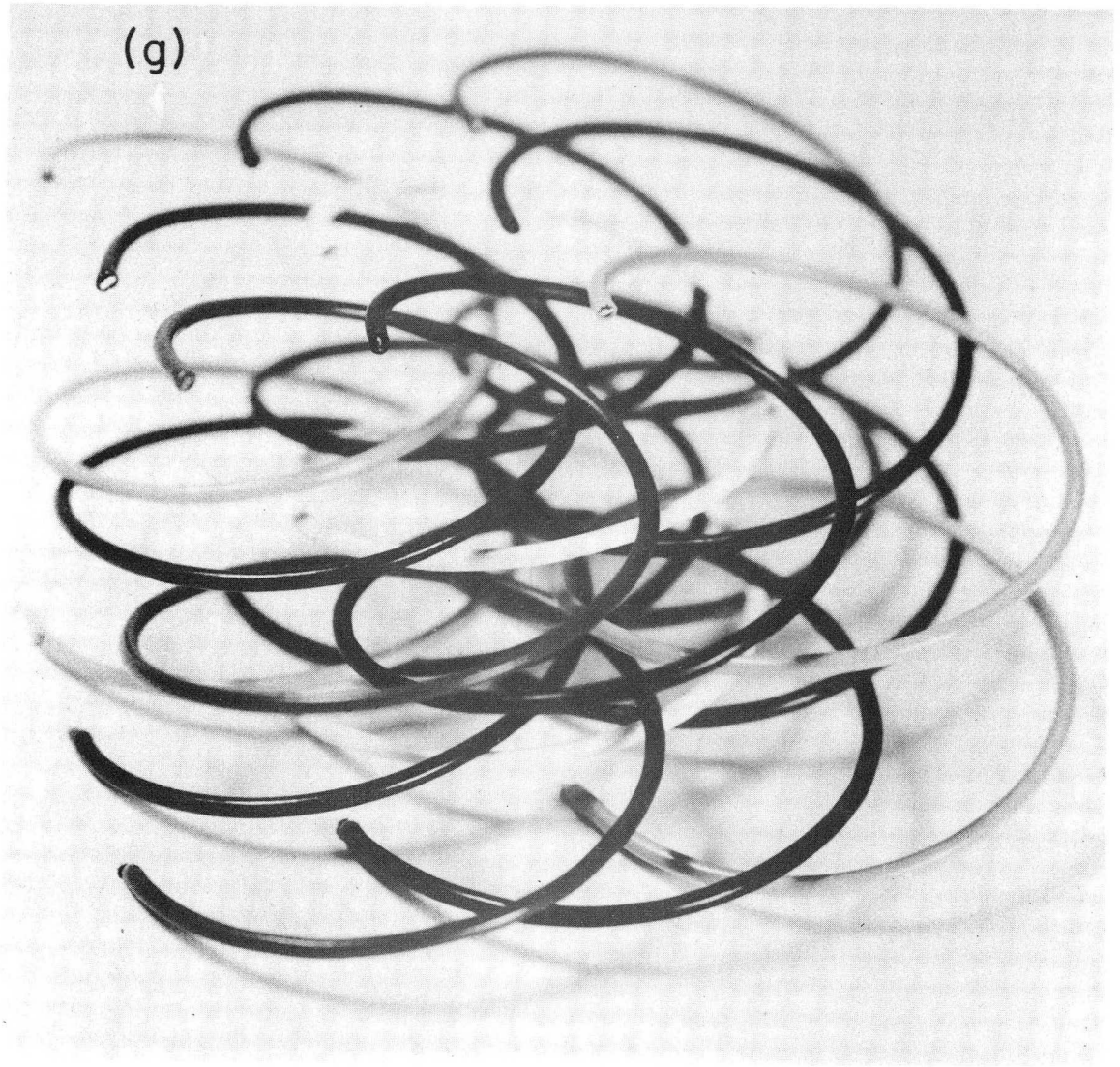

XBB 708-3613

Fig. 2g

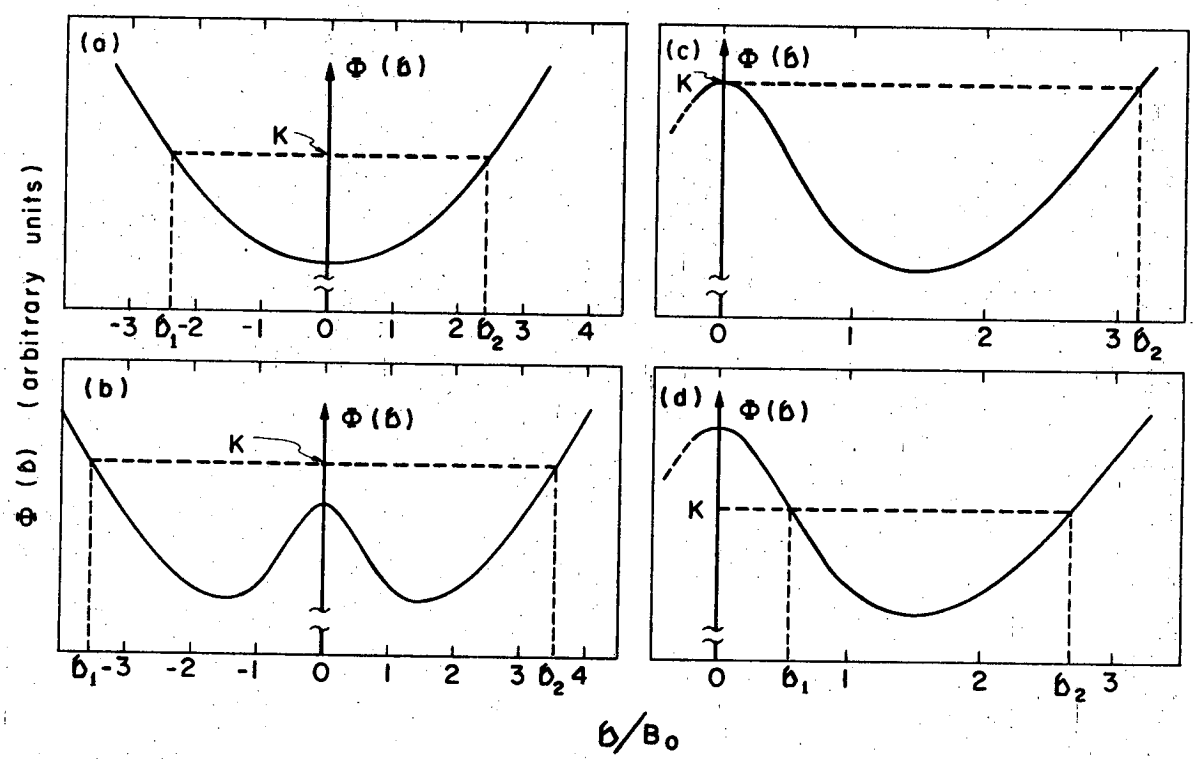

XBL708-3683

Fig. 3.

LEGAL NOTICE

This report was prepared as an account of Government sponsored work. Neither the United States, nor the Commission, nor any person acting on behalf of the Commission:

A. Makes any warranty or representation, expressed or implied, with respect to the accuracy, completeness, or usefulness of the information contained in this report, or that the use of any information, apparatus, method, or process disclosed in this report may not infringe privately owned rights; or

B. Assumes any liabilities with respect to the use of, or for damages resulting from the use of any information, apparatus, method, or process disclosed in this report.

As used in the above, "person acting on behalf of the Commission" includes any employee or contractor of the Commission, or employee of such contractor, to the extent that such employee or contractor of the Commission, or employee of such contractor prepares, disseminates, or provides access to, any information pursuant to his employment or contract with the Commission, or his employment with such contractor.

TECHNICAL INFORMATION DIVISION
LAWRENCE RADIATION LABORATORY
UNIVERSITY OF CALIFORNIA
BERKELEY, CALIFORNIA 94720